# CONCEPTUAL STUDY OF NEUTRON IRRADIATOR DRIVEN BY ELECTRON ACCELERATOR

**D. Ridikas**[1]**, H. Safa, M.-L. Giacri**

CEA Saclay, DSM/DAPNIA/SPhN, F–91191 Gif-sur-Yvette, France

## Abstract

Spallation neutron sources, though very effective in neutron production, are large, expensive and presently would involve certain difficulties in their operation (e.g., beam trips). Contrary, an electron driver, although much less effective in neutron production, is rather cheap and compact machine that, at the same time, might bring advantages in terms of reliability. Here we investigate the use of an external neutron source (irradiator) driven by an electron accelerator. A schematic layout and design of a compact neutron irradiator is proposed with its neutronics and safety being analyzed and discussed in detail. The system is based on a spherical geometry with an electron beam interacting with the target-envelope. Neutrons are produced in the natural or enriched uranium by photonuclear reactions. The system is well sub-critical ($k_{eff}$ < 0.8) and uranium enrichment is below 20%. Neutron balance is optimized by using different geometry and material configurations. Our preliminary calculations show that variable (up to 10% thermal and/or up to 30% with energies higher than 1 MeV) neutron fluxes of a few $10^{14}$ n $s^{-1}$ $cm^{-2}$ could be obtained for different irradiation purposes. An electron machine of ~8 MW power and 100 MeV incident energy should be sufficient to produce external neutrons to drive the system.

[1] Corresponding author's e-mail: ridikas@cea.fr; tel.: +33 1 69087847, fax: +33 1 69087584.

## Introduction

Recently, a world-wide interest in photonuclear processes is experienced, what is motivated by a number of different applications such as shielding problems of medical or fundamental research accelerators, the need of new cost effective neutron sources, transmutation of nuclear waste either directly by photons [1] or by neutrons created from photonuclear reactions [2], radioactive nuclear beam factories based on photofission [3], etc. For a long time photonuclear processes were neglected by particle transport codes mainly due to the lack of the evaluated photonuclear data files. In 1996, in order to make up this backlog, IAEA started a coordinated research programme for compilation and evaluation of photonuclear data for applications. As a result of this effort, a photonuclear data file in ENDF format for 164 isotopes became available in 2000 [4]. One of the first attempts to benchmark these new data files have been performed recently with well known Monte Carlo codes as MCNPX [5] and MCNP [6], enhanced with a photonuclear capability independently by LANL (US) [7] and KFKI (Hungary) [8].

In this paper an unusual system to produce neutrons for irradiation purposes is described eliminating most of the potential difficulties encountered in conventional ADS. The accelerator is an electron machine, being cheaper, more reliable and more compact than high energy high power proton linac. Neutron are produced in a natural or enriched uranium target by photonuclear rather than spallation process. A schematic layout and design of a compact neutron irradiator is proposed with its neutronics and safety being analyzed and discussed in detail. In all calculations we employ already benchmarked MCNP code enhanced with photonuclear capability [8] together with the recommended IAEA photonuclear data files [4].

## Neutron yield and cost

Photonuclear reactions as (?,n) and (?,2n) can be induced in any material by specific gamma rays exciting the Giant Dipole Resonance (GDR) of the nuclei, while (?,fiss) may occur only in the case of actinides. For example, in the case of $^{238}U$ a maximum fission probability of 160 mb can be obtained for photons having energy around 15 MeV. Unfortunately, the most common way for producing high gamma fluxes in the GDR region is the bremsstrahlung process resulting from electrons passing through the matter. This process has a cross section linear with energy above 20 MeV. The resulting bremsstrahlung spectrum is widely spread in the energy range from zero to the incident energy of electron, and only a small fraction of these photons are ``useful" photons, i.e. lying in the GDR range of 15±5 MeV. Therefore, the overall efficiency of neutron production is much lower than one might expect by having in mind the direct photonuclear process.

Let us take an example. The number of fissions per incident electron impinging on an infinite natural uranium target approximately follows a linear law with a threshold energy about 8.5 MeV [2,3]:

$$N_{[fiss/e-]} = 1.9 \text{ x } 10^{-4} (E_{[in\ MeV]} - 8.5).$$

In other words, an electron having an energy of 100 MeV will induce ~0.017 fissions. The neutron production efficiency can then be estimated taking into account that each fission will release about ? = 3.4 prompt neutrons in addition to the contribution of other photonuclear reactions as (?,n) and (?,2n), which contribute nearly the same number of neutrons as the photofission process [2,3]. The total number of neutrons produced for a 100 MeV electron is then ~0.11 n/e. In this case the neutron cost is about 900 MeV. This is much larger than the neutron produced by the spallation process (e.g., a 1 GeV proton on lead target), where each proton can create about 30 neutrons. Here the neutron cost is around 30 MeV, i.e. ~30 times cheaper than the photonuclear one. On the other hand, even the neutron cost is higher, the accelerator cost is much lower in the case of electron machine. Therefore, for the same neutron flux required, a higher electron intensity (and beam power) will be needed due to the lower efficiency. Thus, above a given neutron flux, the spallation will be preferred while for the lower fluxes, the photonuclear process will tend to be cheaper. This is illustrated in Fig. 0, where for a given neutron flux, both an electron machine as well as a proton accelerator has been cost effectively estimated. Note that this is only machine cost, which does not include manpower or buildings(which again are certainly cheaper for the electron machine). In brief, for neutron source intensity higher than $10^{17}$n/s, the spallation process will start to appear more effective, while below this value the photonuclear process is favored.

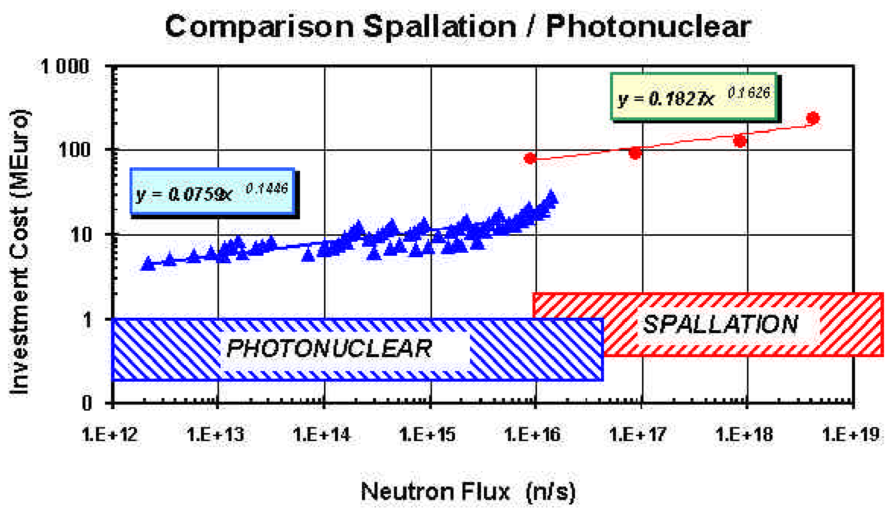


*Figure 0. Spallation versus photonuclear process for neutron production [2].*

**Modelling procedure and geometry considerations**

A simplified model of the neutron irradiator has been created using a typical MCNP [6] geometry setup in 3D. MCNP was also used to obtain the $k_{eff}$ eigenvalues and neutron fluxes. Neutron production with electrons was modeled by the same MCNP code enhanced with photonuclear capability [8]. In all cases the recommended IAEA photonuclear data files have been used [4]. Both (?,n), (?,2n) and (?,fiss) reactions were taken into account explicitly for all materials used in the problem and with a corresponding full secondary neutron transport.

Below we present two different geometry configurations, although in both cases the neutron production target is a spherical uranium envelope. The major difference between them is that in one case electrons interact with the target from inside, while in the second case – from outside as explained in more detail below.

***Spherical geometry G1***

A proposed electron target is 2 cm thick and made of enriched uranium (~19g/cm$^3$). Its total volume and mass is ~17000cm$^3$ and ~323kg respectively. An electron beam is dispersed at the entrance of the system, so it can interact with nearly half of the actual surface of the inner uranium envelope as shown in Fig. 1. We choose 100 MeV electrons since neutron production is nearly linear as a function of the incident beam energy, i.e. neutron production is constant for a given beam power as discussed above. Our major observable is the neutron flux in the central sphere with its radius of 5 cm ("n-flux zone" in Fig. 2). The optimization of the system is done by testing different reflector-moderator materials and different enrichment of uranium target.

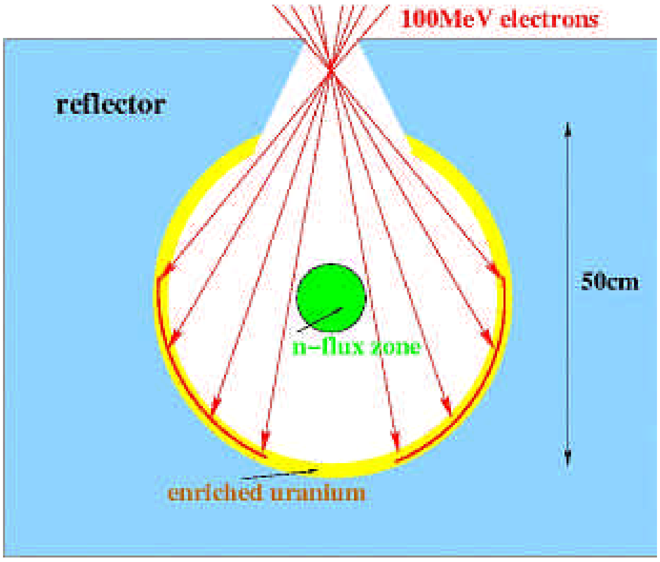


*Figure 1. A simplified geometry (G1) of the neutron irradiator driven by an electron accelerator. See Table 1 for details.*

| Zone Name | Radius (cm) $R_i$-$R_{i+1}$ | Thickness (cm) | Material Composition |
|---|---|---|---|
| *n-flux zone* | *0-5* | 5 | *Irrad. Sample* |
| e-beam zone | 5-25 | 20 | Void |
| u-blanket | 25-27 | 2 | Enriched U (<20%) |
| Reflector | 27-127 | 100 | C or Pb or Be or $D_2O$ |

*Table 1. Neutronics model: zone dimension and material compositions for a neutron irradiator driven by an electron accelerator. Also see Fig. 1.*

As long as we use the target made of enriched uranium, surrounded by moderator-reflector, $k_{eff}$ becomes an important parameter of the system. There are at least two points to be mentioned. Obviously, (a) higher $k_{eff}$ is higher neutron flux in the n-flux zone will be due to the neutron multiplication factor ~1/(1-$k_{eff}$). On the other hand, (b) $k_{eff}$ should be well below one even in accidental situations (e.g., break of the target wall and reflector filling the inner part of the sphere). We suppose that the system can operate safely with $k_{eff}$ ~ 0.80, while $k_{eff}$ ~ 0.95 is the maximal value in the case of the inner wall failure. These two conditions have defined very precisely the maximum enrichment of the uranium target what is presented in Table 2 together with the corresponding $k_{eff}$ values. In addition, the uranium enrichment of 20% we consider being the maximum allowed value for this type of application. Major neutronics parameters of the system with different reflector-enrichment combinations are presented in Table 3.

There is a number of important points which have to be emphasized. First of all, the presence of reflector is indispensable to reduce the neutron leakage. In addition, with a help of an effective reflector the enrichment of uranium may be decreased considerably, while still giving a desired

| Reflector Material | U enriched by (%) | $k_{eff}$ |
|---|---|---|
| *No reflector* | *20.0* | *0.26* |
| **Heavy water (*)** | **0.0** | **0.14** |
| Heavy water | 1.5 | 0.82 |
| Beryllium | 2.0 | 0.80 |
| Natural carbon | 5.0 | 0.82 |
| Natural lead | 20.0 | 0.67 |

*Table 2. Operational $k_{eff}$ as a function of reflector materials and different uranium enrichment.*

| Reflector Material | $M_n$ (%/e) | (?,fiss) (%/e) | (n,fiss) (%/e) | $F_n$ ($n/cm^2/e$) | $F_n$ % ($E_n$<1 eV) | $F_n$ % ($E_n$>1MeV) |
|---|---|---|---|---|---|---|
| *No reflector* | *7.1* | *1.4* | *0.7* | *2.1e-5* | *0.0* | *52.4* |
| **Heavy water (*)** | **8.0** | **1.3** | **0.6** | **7.0e-5** | **29.0** | **15.1** |
| Heavy water | 8.0 | 1.3 | 14.4 | 2.6e-4 | 10.0 | 17.1 |
| Beryllium | 7.8 | 1.3 | 12.6 | 3.0e-4 | 5.4 | 16.6 |
| Natural carbon | 7.1 | 1.4 | 11.8 | 2.6e-4 | 1.4 | 19.9 |
| Natural lead | 7.7 | 1.4 | 6.6 | 1.9e-4 | <<1.0 | 19.5 |

*Table 3. Neutronics of the system (normalized per incident electron). $M_n$ stands for neutron production efficiency per incident electron due to photonuclear reactions, while $F_n$ is a total volumetric flux in the "n-flux zone" of 10 cm diameter (see Table 2 for uranium enrichement values and Fig. 1 for geometry). Heavy water (*) is the case with pure $^{238}U$.*

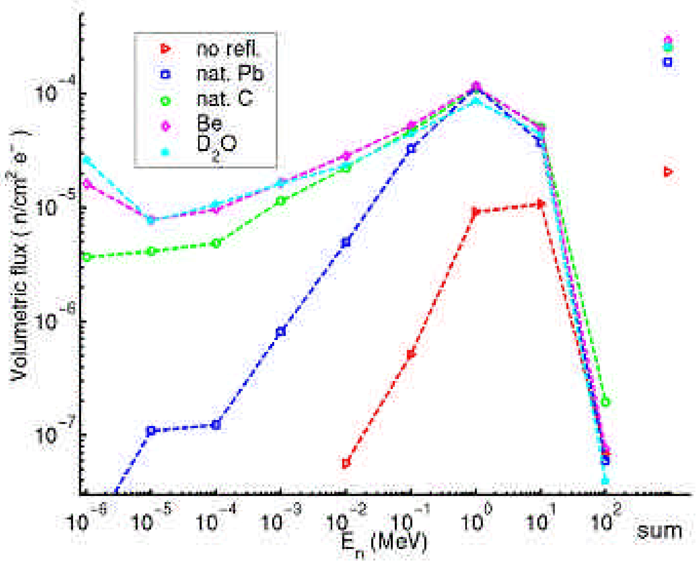


*Figure 2. Neutron energy spectra as a function of different reflector material. The estimated flux corresponds to the average volumetric flux in the n-flux zone (see Fig. 1).*

neutron flux intensity in the irradiation zone of our interest (see column "$F_n$" in Table 3). Secondly, the reflector will play the role of a moderator, so one can really profit the presence of $^{235}U$ in the target. Finally, different reflector materials will have different moderation characteristics, what results in different thermalization level of the flux in the n-flux zone as discussed below. Figs. 2-3 summarizes the consequences as above.

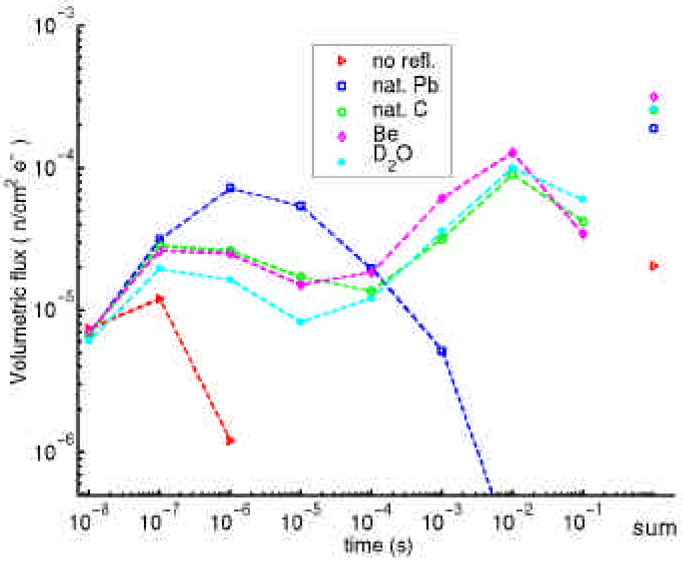


*Figure 3. Neutron time dependence as a function of different reflector material. The estimated flux corresponds to the average volumetric flux in the n-flux zone (see Fig. 1).*

As it is shown in Fig. 2, by placing more efficient reflector material one may increase considerably both the absolute value of the neutron flux (by a factor of ~15 as well as the contribution of thermal neutrons (from ~0% to ~10%). A contribution of fission neutrons due to $^{235}U$ is easily seen from the neutron time dependence presented in the Fig. 3. In the time range from 1e-8 to 1e-5 s neutrons had not enough time to be thermalized. After that (on their way back from the reflector to the target) they will not only contribute to the thermal part of the total neutron flux but also will create secondary fast fission neutrons via neutron induced fission on $^{235}U$ (see the increment of neutron flux in the time range from 1e-4 to 1e-1 s). In this case photoneutrons will contribute less than 20% to the total neutron flux in the n-flux zone (see Table 3 for details).

***Spherical geometry G2***

Similarly like in the first geometry presentation G1, here we consider a neutron production target made of either natural or enriched metallic uranium (~19g/cm$^3$ and 2 cm thick). However, now its total volume and mass is nearly by a factor 5.5 smaller, namely ~3050 cm$^3$ and ~58kg respectively. This is possible only because electrons are interacting from outside of the target. An electron beam is dispersed on the uranium sphere, so it can interact with nearly half of the actual surface of outer envelope as shown in Fig. 4. An important difference (compared to the G1 geometry) is that the beam electrons first should penetrate heavy water before they can interact with uranium. For this reason neutron production becomes not any longer linear as a function of the incident beam energy. As a matter of fact, the optimal performance will be obtained for a given thickness of the moderator at given electron energy (see Table 5 for details). Like in the previous case, our major observable is the neutron flux in the central sphere with its radius of 5cm ("n-flux irradiation zone" in Fig. 4). The characterization of the system is done by testing different reflector-moderator thickness, enrichment of uranium target and incident electron energy.

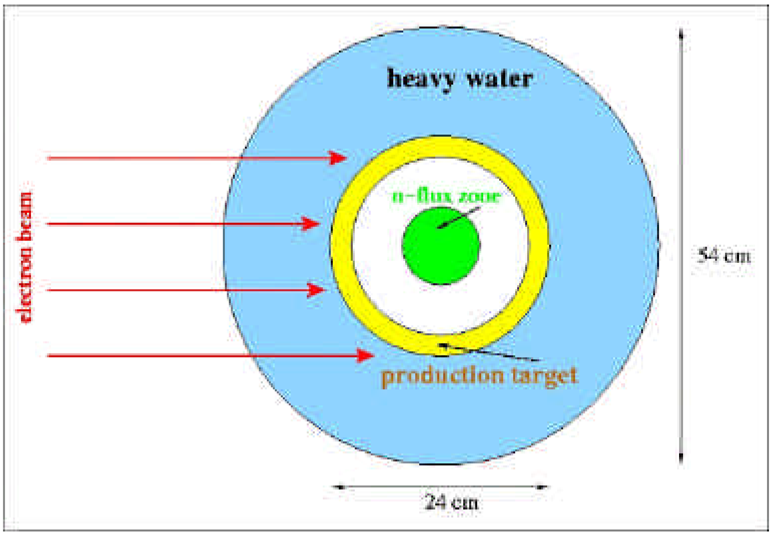


*Figure 4: A simplified geometry (G2) of the neutron irradiator driven by an electron accelerator. See Table 4 for details.*

| Zone Name | Radius (cm) $R_i$-$R_{i+1}$ | Thickness (cm) | Material Composition |
|---|---|---|---|
| *n-flux zone* | *0-5* | *5* | *Irrad. Sample* |
| void zone | 5-10 | 5 | Void |
| u-blanket | 10-12 | 2 | natural or enriched U (<20%) |
| Reflector * | 12-A; A = [12 37] | B; B = [0 25] | $D_2O$ |

*Table 4. Neutronis model: zone dimension and material compositions for a neutron irradiator driven by an electron accelerator. Also see Fig. 4. Note that the the thickness of heavy water zone is a parameter of optimization.*

| $D_2O$ Thickness, (cm) | $E_e$ = 100 MeV | | $E_e$ = 200 MeV | |
|---|---|---|---|---|
| | $M_n$, (%/e) | $F_n$, (n/cm$^2$/e) | $M_n$, (%/e) | $F_n$, (n/cm$^2$/e) |
| 0 | 8.8 | 1.3e-4 | 17.0 | 2.5e-4 |
| 5 | 7.9 | 1.8e-4 | 16.8 | 4.0e-4 |
| **10** | **7.2** | **2.0e-4** | 16.0 | 4.5e-4 |
| **15** | 6.5 | 1.9e-4 | **15.5** | **4.8e-4** |
| 20 | 5.6 | 1.7e-4 | 14.7 | 4.7e-4 |
| 25 | 4.6 | 1.4e-4 | 13.5 | 4.4e-4 |

*Table 5. Neutronics of the system (normalized per incident electron) as a function of reflector thickness and incident electron energy. Here in all cases 2cm thick natural uranium was used.*

After a number of optimization calculations were finished, we selected five, in our opinion, the most representative cases for a more detailed analysis. The corresponding results are summarized in Table 6 and Figs. 5-6. Note that in the case No 5 we have also divided all results by a factor of two. This is simply because of two times higher incident electron energy used when compared to the cases 1-4. In this way all results can be easily scaled to the same incident beam power for 100 MeV electrons.

| Configuration No And description | $M_n$ %,e | (?,fiss) %/e | (n,fiss) %/e | $F_n$ $n/cm^2/e$ | $F_n$ % ($E_n$<1eV) | $F_n$ % ($E_n$>1MeV) |
|---|---|---|---|---|---|---|
| **1)** $E_e$ = 100 MeV; $d(D_2O)$ = 0 cm $^{238}U$ 100% | 8.8 | 1.7 | 0.6 | 1.2e-4 | 0.0 | 56.0 |
| **2)** $E_e$ = 100 MeV; $d(D_2O)$ = 10 cm $^{238}U$ 100% | 7.4 | 1.4 | 0.5 | 2.0e-4 | 2.9 | 28.8 |
| **3)** $E_e$ = 100 MeV; $d(D_2O)$ = 20 cm $^{238}U$ 100% | 5.6 | 1.0 | 0.4 | 1.7e-4 | 10.4 | 24.8 |
| **4)** $E_e$ = 100 MeV; $d(D_2O)$ = 20 cm $^{238}U$ 80% & 20% $^{235}U$) | 5.7 | 1.1 | 4.2 | 3.2e-4 | 1.2 | 29.8 |
| **5)** $E_e$ = 200 MeV; $d(D_2O)$ = 15 cm $^{238}U$ 100% | 15.5 | 2.9 | 1.1 | 4.8e-4 | 6.8 | 27.9 |
| 5) x 0.5 (see text for details) | 7.8 | 1.5 | 0.6 | 2.4e-4 | | |

*Table 6. Neutronics of the system (normalized per incident electron) as a function of different configurations.*

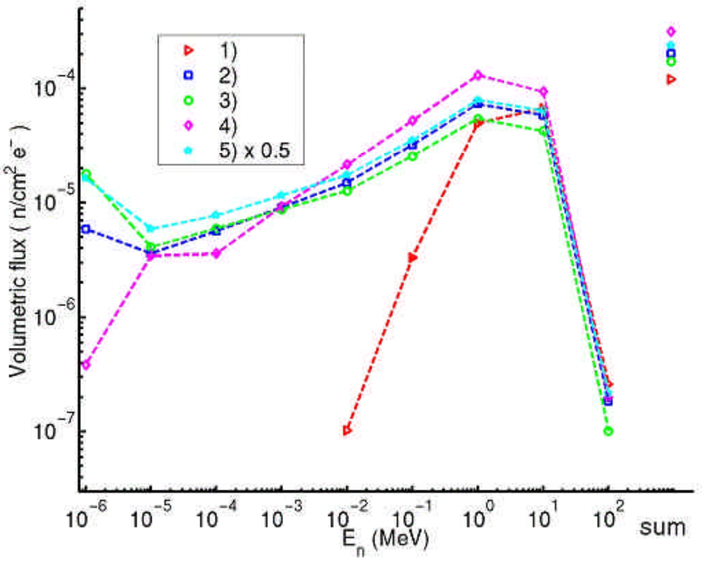


*Figure 5. Neutron energy spectra as a function of different reflector material. The estimated flux corresponds to the average volumetric flux in the n-flux zone (see Fig. 4).*

Like in the case of the geometry G1 a number of important findings should be pointed out. First of all, the presence of a reflector is indispensable to reduce the neutron leakage. Although it decreases slightly (by a factor of 1.2) the primary neutron production $M_n$ (compare case No1 and No2 in Table 6), the total neutron flux $F_n$ is increased by a factor of 1.7. In addition, by varying reflector thickness one can create variable neutrons fluxes (see Fig. 5), say, up to 10% thermal (case No3). As soon as neutrons become in part thermalized, one can also profit the presence of $^{235}U$ in the target (see Table 6 and Figs. 5-6 for the case No 4). A contribution of fission neutrons due to ($n_{th}$ + $^{235}U$) now is easily seen from the neutron time-dependence presented in Fig. 6. In the time range from 1e-8 to 1e-5 s neutrons had not enough time to be thermalized. After that (on their way back from the reflector to the target) they will not only contribute to the thermal part of the total neutron flux (ceases 3 and 5) but also will create secondary fast fission neutrons (see the increment of neutron flux in the time range from 1e-4 to 1e-2 s). In this case the external source and secondary neutron production will contribute almost equally ($k_{eff}$ ~ 0.5) to the total neutron flux in the n-flux zone (see Table 6 for details). Finally, the case No 5 shows that higher electron energies are favored to improve the system's performance. This is clearly seen by comparing the case (No5 x 0.5) with the case No2. As we mentioned earlier, higher energy is preferred since electrons still have to pass the moderator region before interacting with uranium.

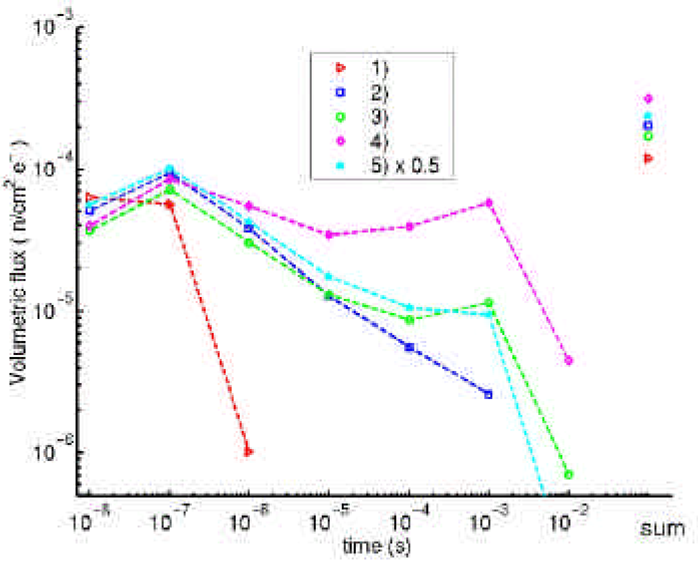


*Figure 6. Neutron time dependence as a function of different reflector material. The estimated flux corresponds to the average volumetric flux in the n-flux zone (see Fig. 4).*

**Discussion**

From Tables 3 and 6 one can conclude that the geometry G2 is more attractive than G1. Although the performance of the system is comparable in both cases, G2 is much more compact, uses less uranium (by a factor of 5.5) and not necessarily needs target enrichment by $^{235}U$. By changing the thickness of heavy water neutron thermalization level can vary from 0 to 10 %, what makes the system rather flexible. In addition, some of the beam power will be dissipated directly in the $D_2O$ before even reaching the uranium target, e.g. up to 50% in the configuration No 3 (see Table 6). This fact , together with others mentioned above, is an important advantage, since the production target is supposed to withstand beam power of a few MW as discussed below.

So what are the electron accelerator requirements? Let us assume that our goal is to have a neutron flux of the order of $10^{14}$ n $s^{-1}$ $cm^{-2}$ to be compatible with a typical experimental reactor installation. It is easy to estimate with a help of Tables 3-6 that in this case one would need an incident 100MeV electron beam (current) of the order of ~8 MW (80mA), i.e. as many as ~$5x10^{17}$ pps. Working with even higher beam power might be not an easy task due to the target heat dissipation. We note that the electron target will be heated not only by the incident beam (a few MW) but also by a non negligible fission power (up to 1 MW). This results in the total average power density of, say, 0.5 - 1.5 kW/$cm^3$ (depending on the configuration) deposited in the uranium target. In our opinion, this value could still be tolerated but going much further might become difficult if not technologically impossible. In any case, it is also clear that this situation favors a liquid reflector-moderator, which could be used as a coolant at the same time. More detailed study on the target heating-cooling is definitely needed. In addition, one should also make an estimate for how long the target could operate in nominal operation conditions. Finally, we would like to mention that the radioprotection and non-proliferation issues should be addressed separately.

**Conclusions**

A non-conventional ADS system has been proposed to produce neutrons via photonuclear reactions. It includes an electron accelerator and a spherical natural or enriched uranium target-blanket (2 cm thick) surrounded by a reflecting material. The system is well sub-critical ($k_{eff}$<0.8) and uranium enrichment is below 20%. Very encouraging preliminary calculations have been performed using the MCNP code enchanced with a photonuclear capability. It is shown that variable (from 0 to 10% thermal) neutron fluxes of a few $10^{14}$ n $s^{-1}$ $cm^{-2}$ could be obtained for different irradiation purposes. Nearly 30% of these neutrons have energies higher than 1 MeV. The electron machine at ~8 MW power and 100 MeV incident energy should be sufficient to produce external neutrons to drive the system. This results in the total average power density of ~1.5 kW/$cm^3$ deposited in the target, perhaps being the limiting factor. More detailed calculations related to safety and heat dissipation issues are in progress and will be reported elsewhere.

**References**

[1] T. Matsumoto, "Calculation of Gamma Ray Incineration of $^{90}$Sr and $^{137}$Cs", *Nucl. Instr. & Methods in Phys. Res.* **A 268** (1988) 234; D. Ridikas and M.-L. Giacri, "Transmutation of $^{237}$Np in high intensity photon fluxes", in preparation for publication (October 2002).

[2] B. Bernardin, D. Ridikas, H. Safa, ``A Prototype Sub-critical Reactor Driven by Electron Accelerator", Proc. of the Int. Conf. on Accelerator Applications/Accelerator Driven Transmutation Technology and Applications (AccApp/ADTTA'01), 12-15 November 2001, Reno, Nevada, USA; D. Ridikas, H. Safa, B. Bernardin, "A Prototype Beta Compensated Reactor (BCR) Driven by Electron Accelerator", Proc. of the Int. Conf. *PHYSOR 2002, Seoul, Korea, October 7-10, 2002*

[3] H. Safa and D. Ridikas, "Photofission for the SPIRAL-2 Project", Proc. of the Int. Conference on Isotope Separation On Line (ISOL'01), 11-14 March, 2001, Oak Ridge, USA.

[4] IAEA, "Handbook on photonuclear data for applications", IAEA TEC-DOC Draft No3, March 2000.

[5] L.S. Waters, "MCNPX™ USER's MANUAL", Los Alamos National Laboratory, preprint TPO-E83-G-UG-X-00001 (November 1999); also see http://mcnpx.lanl.gov/.

[6] J. Briesmeister for Group X-6, "MCNP-A, A General Monte Carlo Code for Neutron and Photon Transport", Version 4A, LANL, preprint LA-12625-M (1993).

[7] M.C. White, R.C. Little and M.B. Chadwick, "Photonuclear Physics in MCNP(X)", Proceedings of the 3rd International Topic Meeting on Nuclear Applications of Technology, Long Beach, California, November 14-18, 1999, ANS, 515 (1999).

[8] P. Vertes and D. Ridikas, "Some Test Calculations with the IAEA Photonuclear Data Library", Proc. the Int. Conference on Nuclear Data for Science and Technology (ND2001), October 7-12, 2001, Tsukuba, Ibaraki, Japan; in print by *Nuclear Science and Technology.*